

Article

# Magnetic Fields and Halos in Spiral Galaxies

Marita Krause

Max-Planck-Institut für Radioastronomie, Auf dem Hügel 69, 53121 Bonn, Germany;  
mkrause@mpifr-bonn.mpg.de

Received: 18 February 2019; Accepted: 18 April 2019; Published: 4 May 2019



**Abstract:** Radio continuum and polarization observations reveal best the magnetic field structure and strength in nearby spiral galaxies. They show a similar magnetic field pattern, which is of spiral shape along the disk plane and X-shaped in the halo, sometimes accompanied by strong vertical fields above and below the central region of the disk. The strength of the total halo field is comparable to that of the disk. The small- and large-scale dynamo action is discussed to explain the observations with special emphasis on the rôle of star formation on the  $\alpha - \Omega$  dynamo and the magnetic field strength and structure in the disk and halo. Recently, with RM-synthesis of the CHANG-ES observations, we obtained the first observational evidence for the existence of regular magnetic fields in the halo. The analysis of the radio scale heights indicate escape-dominated radio halos with convective cosmic ray propagation for many galaxies. These galactic winds may be essential for an effective dynamo action and may transport large-scale magnetic field from the disk into the halo.

**Keywords:** galaxies: spiral; galaxies: magnetic fields; galaxies: halos; galaxies: star formation; galaxies: galactic winds; galaxies: evolution; radio continuum: galaxies

## 1. Introduction

The effects of magnetic fields on the physical processes in spiral galaxies, their disk-halo interaction and their evolution have been frequently neglected in the past. Within the last 20 years, with increasing computing facilities, some authors included them in their simulations of, e.g., the interstellar medium and disk-halo interaction (e.g., [1,2]) or in the evolution of spiral galaxies (e.g., [3]). Their result is that magnetic fields play an important role, even if the magnetic and cosmic ray energy density in the interstellar medium is small compared to that of the rotation. The magnetic field energy density is indeed comparable to that of the turbulent gas motion and much higher than that of the thermal gas, as has been determined for the nearby galaxies NGC 6946 [4] and M33 [5]. Hence, magnetic fields are dynamically important in the processes of the interstellar medium. Direct comparison of three-dimensional MHD simulations of an isolated galaxy with and without a magnetic field show that a magnetic field leads to a lower star formation rate at later times, it reduces the prominence of individual spiral arms and it causes weak outflows from the disk up to several kpc above and below the disk [3]. These results have been supported by cosmological magnetohydrodynamical simulations of galaxies in clusters [6] and will be further researched for isolated Milky Way-like galaxies in dark halos, e.g., with the Auriga Project [7,8].

Observationally, the magnetic field in external galaxies can be best studied in the radio continuum emission in the centimeter-wavelength range. The total intensity of the synchrotron emission gives the strength of the total magnetic field. The linearly polarized intensity reveals the strength and the structure of the resolved *ordered* field in the sky plane ( $B_{\perp}$ , i.e., perpendicular to the line of sight (LOS)). However, the observed polarization vectors suffer from Faraday rotation and depolarization (i.e., a decrease of the degree of linear polarization when compared to the intrinsic one) on the way from the radiation's origin to us. Correction for Faraday rotation is possible with observations at different

wavelengths by determining the rotation measure RM (being proportional to  $\int n_e B_{\parallel} dl$  where  $n_e$  is the thermal electron density and  $B_{\parallel}$  the magnetic field strength parallel to the line of sight  $l$ ). The rotation measure itself can be used to correct the observed polarization angle and also to estimate the strength of  $B_{\parallel}$  if the thermal electron density can be estimated from the emission measure EM as determined from H $\alpha$  or X-ray observations of the galaxy. The key point is that the sign of the RMs gives the *direction* of the parallel magnetic field component. The field strength of both components, parallel and perpendicular to the LOS, together with the information of the intrinsic polarization vectors enables us in principle to get a three-dimensional picture of the magnetic field.

## 2. Faraday Rotation and Depolarization Effects

While the polarized intensity gives the *orientation* of the magnetic field, the magnetic field *direction* can only be determined by the Faraday rotation measure. As the polarization is only sensitive to the magnetic field orientation, the polarization angle can only be determined with an  $\pm n \cdot \pi$  ambiguity. A regular pattern of the intrinsic magnetic field vectors deduced from the observed polarized intensity may indicate a large-scale magnetic field but can also originate from anisotropic turbulent magnetic fields, e.g., compressed fields with opposite directions. However, as anisotropic turbulent magnetic fields have different directions along the LOS, the differential RMs along the LOS have different signs and at least partly cancel along the LOS. Only the detection of RMs of reasonable strengths along the LOS indicates a regular magnetic field component. If, in addition, the different RM observed along different LOS presented in a map have a smooth distribution of regions with positive and negative RM values on scales significantly larger than the beam size, a regular magnetic field is indicated. In this case, the polarization vectors are also expected to be ordered on scales larger than the beam size.

Further, depolarization effects have to be considered. We distinguish between wavelength-independent and wavelength-dependent depolarization. By comparing maps observed at different frequencies but smoothed to the same linear resolution, the observed depolarization is solely due to wavelength-dependent depolarization effects. Several different wavelength-dependent depolarization effects are important to consider: differential Faraday rotation, Faraday dispersion, an RM gradient within the beam, and bandwidth depolarization [9,10]. Faraday dispersion is due to turbulent (random) magnetic fields within the source (internal Faraday dispersion) and between the source and us (external Faraday dispersion), whereas differential Faraday rotation and depolarization by an RM gradient depend on the regular magnetic field within the emitting source. Especially differential Faraday rotation may cause that the source is not transparent in polarization if the internal Faraday rotation reaches values of  $90^\circ$  or more. This is usually the case near the midplane of spiral galaxies seen edge-on observed at decimeter wavelengths and may be even the case in the centimeter-wavelength regime, as observed in NGC 4631 [11]. Otherwise, bandwidth depolarization within a single spectral window for RM-synthesis can usually be neglected with the current broadband multi-channel receivers (e.g., at the JVLA).

Polarized emission effected by differential depolarization can at least partly be recovered by polarization spectroscopy and RM-synthesis [12]. However, even with the present broadband receivers (e.g., with 2–4 GHz bandwidth at C-band of the JVLA), the RM Spread Function (RMSF) is too broad (FWHM  $\approx 2000 \text{ rad m}^{-2}$ ) to resolve different polarizing structures along the LOS within one galaxy. Secondly, RM-synthesis can only analyze that part of an object that is optically thin in linear polarization. Thirdly, even with the present more sensitive and broad-band polarization receivers, we cannot trace the polarized signal much further out into the halo (i.e., the region with faint emission) than previously without this technique, as the sensitivity per polarization window (channel) did not really increase, especially as a signal-to-noise of about 5 is needed for the cleaning procedure of the RMSF sidelobes [13]. Nevertheless, present RM-synthesis observations deliver for the first time a map of the intrinsic magnetic field vectors  $B_{\perp}$  together with a map of Faraday depth (as a measure of  $B_{\parallel}$ ) from observations at one single band (best is C-band for edge-on galaxies, and C-band and possibly S-band for face-on galaxies).

### 3. Magnetic Field Strength and Star Formation

The total magnetic field strength in a galaxy can be estimated from the non-thermal radio emission under the assumption of equipartition between the energies of the magnetic field and the relativistic particles (the so-called *energy equipartition*), as described in Beck & Krause [14]. The mean equipartition value for the total magnetic field strength for a sample of 74 spiral galaxies observed by Niklas [15] is on average  $9 \pm 3 \mu\text{G}$  but reaches locally higher values *within* the spiral arms of up to 20–25  $\mu\text{G}$  in M51 [16]. The strength of the ordered magnetic fields in spiral galaxies are typically 1–5  $\mu\text{G}$ , and may reach locally values up to 10–15  $\mu\text{G}$  as, e.g., in NGC 6946 [4] and M51 [16]. The field strengths in the halo are similar to the those in the disk (see Section 4).

The turbulent magnetic field is typically strongest within the optical spiral arms, whereas the regular fields are strongest in between the optical spiral arms [17], as shown in Figure 1 (left), or at the inner edge of the density-wave spiral arm as seen in M51 [16]. Sometimes, the inter-arm region is filled smoothly with regular fields, in other cases the large-scale field form long filaments of polarized intensity such as in IC342 (Figure 1, right) [18,19] or the so-called *magnetic spiral arms* such as in NGC 6946 [20].

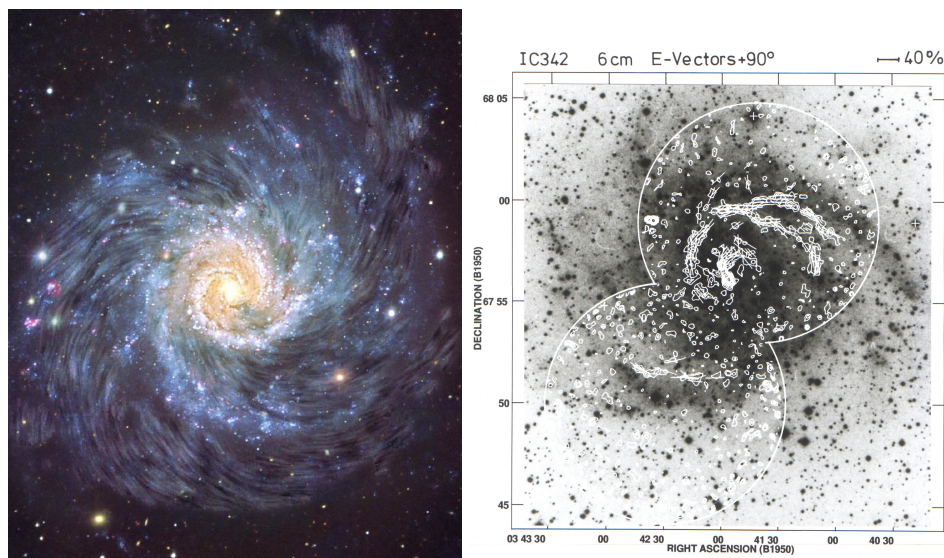


**Figure 1.** (Left) Polarized intensity of the spiral galaxy NGC 628 at  $\lambda$  9.7 cm (3.1 GHz) from JVLA observations with a resolution of  $18''$  HPBW with the magnetic fields illustrated as flow lines, overlaid on an optical image plus  $H\alpha$  from Calar Alto Observatory [17]. (Right) Polarized intensity contours of IC342 at  $\lambda$  6.2 cm (4.8 GHz) from VLA observations with a resolution of  $16''$  HPBW, overlaid on a POSS optical image. The vectors give the apparent magnetic field orientation (i.e., not corrected for Faraday rotation) [18].

Strongly interacting galaxies or galaxies with a high star formation rate (SFR) tend to have generally stronger total magnetic fields. The latter fits to the equipartition model for the radio-FIR correlation Niklas & Beck [21], according to which the non-thermal emission increases  $\propto SFR^{1.3 \pm 0.2}$  and the *total*, mostly turbulent magnetic field strength  $B_t$  increases  $\propto SFR^{0.34 \pm 0.14}$  [22].

No similar simple relation is known for the *ordered* magnetic field strength. Stil et al. [23] integrated the polarization properties in 41 nearby spiral galaxies and found that (independent of inclination effects) the degree of linear polarization is lower ( $<4\%$ ) for more luminous galaxies, in particular those for  $L_{4.8} > 2 \times 10^{21} \text{ W Hz}^{-1}$ . The radio-brightest galaxies are those with the highest SFR. Although dynamo action needs star formation and supernova remnants as the driving force for velocities in vertical direction, we conclude from our observations that stronger star formation reduces the magnetic field regularity. On kpc-scales, Chyży [24] analyzed the correlation between magnetic field regularity

and SFR locally within one galaxy, NGC 4254. While he found that the total and random field strength increase locally with SFR, the ordered field strength is locally uncorrelated with SFR.

#### 4. Magnetic Field Structure in Spiral Galaxies

Observations of spiral galaxies seen face-on reveal a large-scale magnetic field pattern along the plane of the galaxy. The magnetic field lines generally follow a spiral structure with pitch angles from  $10^\circ$  to  $40^\circ$ , which are similar to the pitch angles of the optical spiral arms, as visible, e.g., in Figure 1. Detailed studies showed that the magnetic pitch angles are indeed systematically larger than the spiral arm pitch angles in three face-on spiral galaxies (Frick et al. [25] for M83, Berkhuijsen et al. [26] for M101, and Mulcahy et al. [17] for NGC 628) giving evidence for the action of a large-scale dynamo in these galaxies. The large-scale pattern is accompanied by a small-scale magnetic field that is stronger within the optical spiral arms.

The magnetic field is thought to be amplified and maintained by dynamo action, especially the large-scale structure by the action of the  $\alpha - \Omega$  mean-field dynamo [27], which predicts an axisymmetric mode (ASS) along the galactic plane of the galaxy to be excited most easily. The mean-field dynamo theory alone, however, cannot explain why the strength of the large-scale magnetic field is higher in the inter-arm region (as presented in Section 3) or why the magnetic pitch angles are similar to the pitch angles of the optical spiral arms. Within the dynamo theory, the magnetic pitch angles are simply determined by the ratio of the radial to the azimuthal magnetic field components [27], whereas the spiral arm pitch angle may even be related to the supermassive black hole mass [28].

Observation of spiral galaxies seen edge-on show in general a plane-parallel magnetic field structure along the midplane which is the expected projection of the spiral field in the disk as observed in face-on galaxies. This is also the case in NGC 4631, as detected by Mora & Krause [11].

In the halo, the ordered magnetic field is X-shaped, as indicated in the sketch for NGC 5775 observed with an inclination  $i = 86^\circ$  (Figure 2). In some galaxies, the X-shaped halo field is accompanied by strong vertical components above and/or below the central region, as in NGC 5775 (Figure 2) and NGC 4631 (Figure 3). Until recently, missing RM values within the halos prevented us from deciding observationally whether the halo fields are large-scale regular or ordered fields. They can also be a mixture of both.

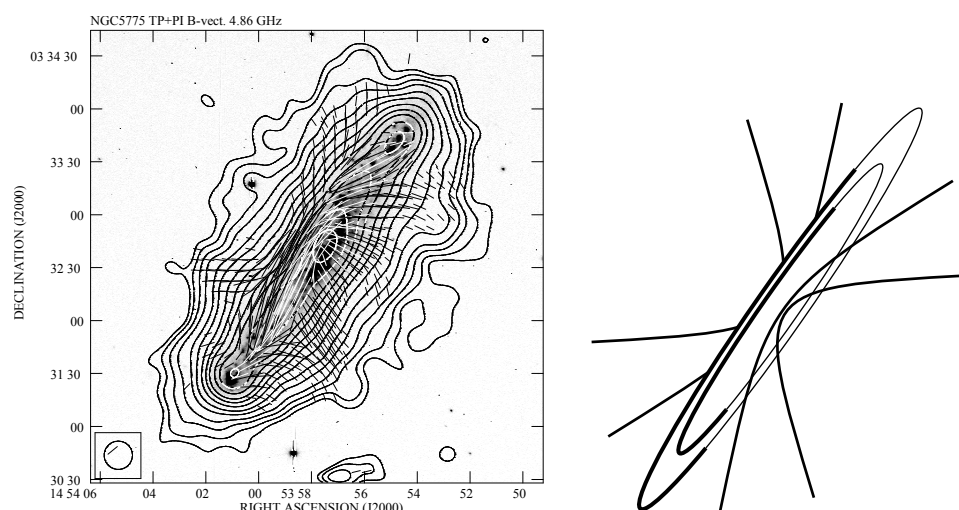


**Figure 2.** Total intensity contours map (left) with apparent magnetic field orientation at 4.8 GHz of NGC 5775 (from the VLA with a resolution of  $16''$  HPBW) overlaid on an  $H\alpha$  image and sketch (right) of a possible regular magnetic field configuration in the disk and in the halo for NGC 5775 [29].

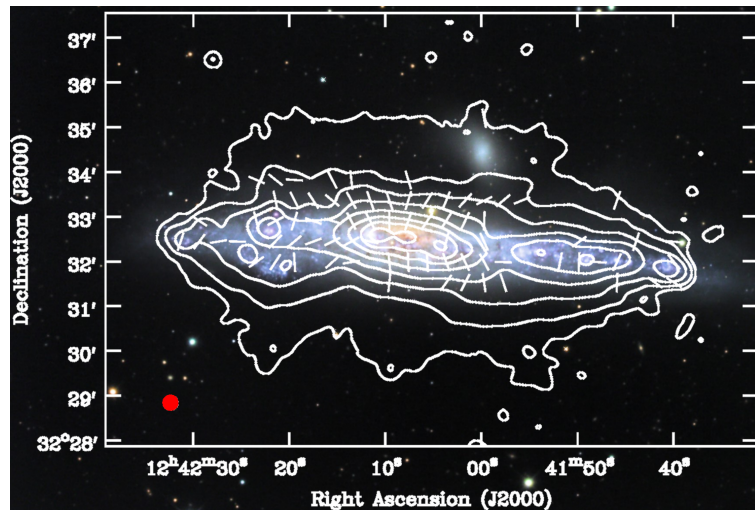


**Figure 3.** Radio continuum emission (contours) of the edge-on spiral galaxy NGC 4631 at 5.99 GHz from combined JVLA and 100-m Effelsberg observations with a resolution of  $20.5''$  HPBW with intrinsic magnetic field orientation, overlaid on a color-scale optical DSS image [30].

This changed recently with the Continuum HALos in Nearby Galaxies–EVLA Survey (CHANG-ES) observations of 35 edge-on spiral galaxies by Irwin et al. [31] (see also [32]). Within this sample, we detected polarized intensity in several edge-on galaxies far into the halo with ordered intrinsic magnetic field vectors and an RM pattern that is regular over several beams sizes. This is the first observational evidence for the existence of regular magnetic fields in the halo. Our analysis shows that these regular magnetic fields have scales  $\geq 800$  pc [33]. The most striking result is observed in NGC 4631, as shown in Figure 4 with a quasi-periodic RM pattern in its northern halo indicating giant magnetic ropes (GMRs) in the halo [34]. A dynamo-based modeling for the halo field in NGC 4631 was proposed by Woodfinden et al. [35] (see also Irwin et al. [32]). However, their assumptions are not generally accepted, as argued by Moss & Sokoloff [36].

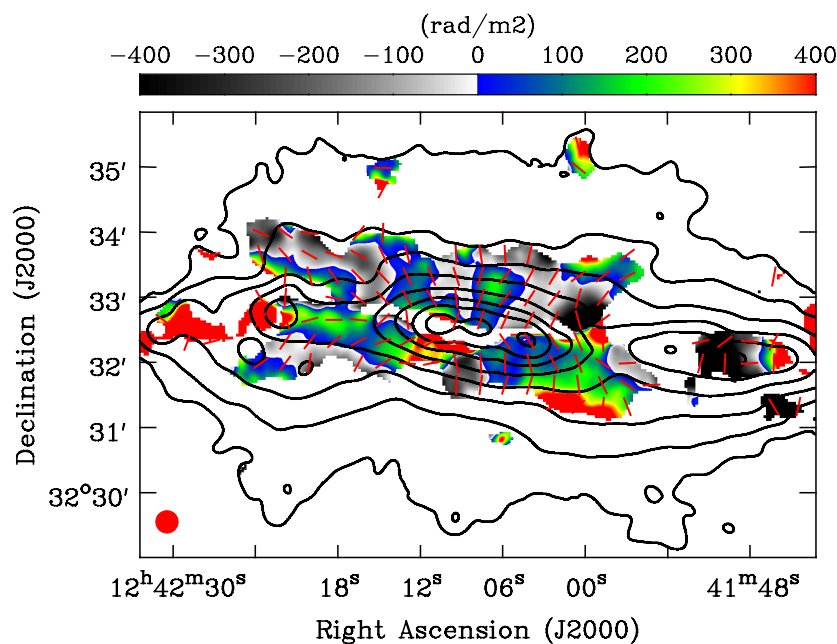


**Figure 4.** RM map of NGC 4631 in color scale as determined from CHANG-ES C-band (JVLA D-configuration) observations with intrinsic magnetic field orientation with  $20.5''$  HPBW resolution [34]. The total intensity contours are the same as in Figure 3.

The total magnetic field strengths has been determined from the total intensity radio maps for many galaxies with the assumption of equipartition [14,37]. It was found that the magnetic field strengths in large parts of the halo are comparable to or slightly lower than the magnetic field strength in the disk outside the central region (as, e.g., in NGC 253 [38], NGC 4631 [30], NGC 891 and NGC 4565 [39], NGC 4666 [40], and NGC 4013 [41], with 5–10  $\mu\text{G}$  within the first few kpc in the halo compared to 6–11  $\mu\text{G}$  in the disk outside the central regions. These relatively strong halo fields cannot be explained alone by the classical mean-field  $\alpha - \Omega$  dynamo operating in the disk (see Section 5). Although the disk field is accompanied by a poloidal halo field, its strength is by a factor of about 10 weaker than the disk field strength. Hence, either there is also dynamo action in the halo or a galactic wind is needed that transports the magnetic field from the disk into the halo. This is further discussed in Section 6.

## 5. Dynamo Action and the Evolution of the Large-Scale Magnetic Field

The large-scale magnetic field can only be amplified and maintained by dynamo action. While a large-scale dynamo is necessary to produce a large-scale magnetic field structure, field amplification alone is faster by the action of a small-scale dynamo [20,42]. For a galactic disk, the large-scale dynamo is the  $\alpha - \Omega$  dynamo, simplified by the mean-field dynamo equations for thin disks. Solution of these equations are the large-scale dynamo modes, with the axisymmetric spiral field structure (ASS) being the dominant mode ( $m = 0$ ), which is generated easiest, followed by the bisymmetric structure (BSS,  $m = 1$ ) and higher modes. The three-dimensional field configurations can be either symmetric (of quadrupole type) or asymmetric (of dipole type) with respect to the galactic plane, where the poloidal field component is about a factor of 10 weaker than the disk field. According to the dynamo theory, the pitch angle of the magnetic field spiral is determined by the dynamo numbers  $R_\alpha$  and  $R_\Omega$  ( $p = \arctan B_r / B_\phi = \arctan(R_\alpha \cdot R_\Omega)^{-1/2}$  for the growing (linear) case [27] and somewhat more complicated for the saturated (nonlinear) case [43]), not by the pitch angle of the gaseous spiral arms. The modes determined observationally in a dozen of nearby galaxies and their relative amplitudes are summarized in [44,45]. The dominating mode in the disk is indeed the ASS, which is of even parity at least for NGC 891 [22] and NGC 5775 [29]. Recently, first indications for a radial magnetic field reversal within the disk of an external galaxy have been observed in NGC 4666 [40].

As part of the SKA design study, we investigated the large- and small-scale dynamo action and the ordering process of the large-scale magnetic field structure during galaxy formation and cosmological evolution [46]. Turbulence generated in protogalactic halos by thermal virialization can drive an effective turbulent (small-scale) dynamo, which amplifies the field strength to energy equipartition with the turbulent gas (beginning at  $z \approx 10$  in Figure 5, left). The large-scale dynamo mainly orders the magnetic field with timescales determined by the mean-field dynamo theory. Hence, the large-scale fields evolve with time. Galaxies similar to, e.g., the Milky Way, formed their disks at  $z \approx 10$ . Regular fields of  $\mu\text{G}$  strength and a few kpc coherence length were generated within 2 Gyr (beginning at  $z \approx 20$  in Figure 5, left), but field ordering on the coherence length of the galaxy size requires additional 6 Gyr for Milky-Way-type galaxies. Dwarf galaxies can already host fully coherent fields at  $z \approx 1$ , while giant disk galaxies may not have reached fully coherent field pattern in the Universe's lifetime up to now [46]. Similar results were attained recently by a semi-analytic galaxy formation model about the evolution of galactic magnetic fields [47].

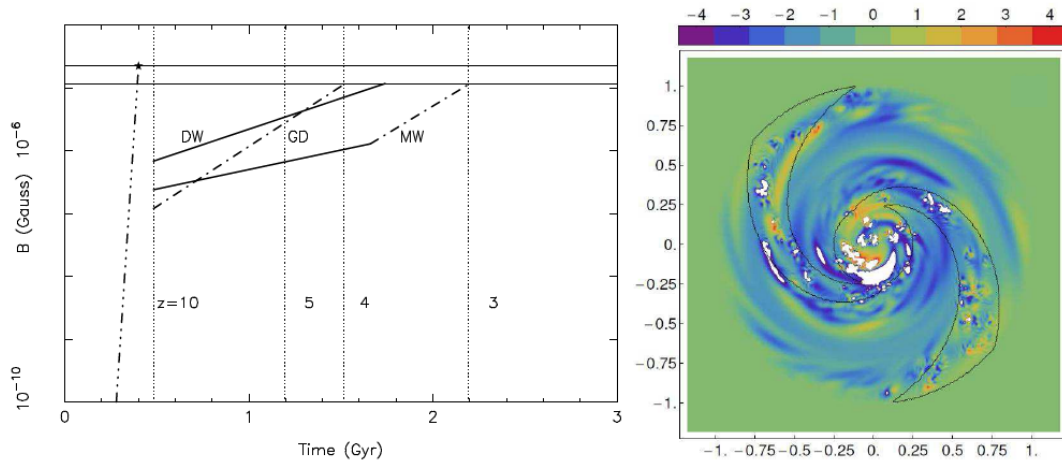


**Figure 5.** (Left) Evolution of magnetic field strength in dwarf galaxies (DW), Milky-Way-type galaxies (MW), and in giant disk galaxies (GD). The thick dashed-dot-dot line shows the evolution of the small-scale magnetic field generated by the small-scale dynamo. The evolution of the large-scale magnetic field generated by the  $\alpha - \Omega$  dynamo in quasi-spherical galaxies are shown by the thick solid line and that in thin-disk galaxies as thick dashed-dot dashed lines [46]. (Right) Color coded image of the modeled azimuthal magnetic field strength in the disk of a spiral galaxy with turbulent magnetic field injection assumed within the normal spiral arm regions as indicated by the thin black lines after 13.2 Gyr. The field strength is given in  $\mu\text{G}$  [48].

The field ordering of a so-called “spotty” magnetic field structure was studied in more detail by Arshakian et al. [49] assuming that the large-scale dynamo starts from coherent fields in spots of 100 pc in size and 0.02  $\mu\text{G}$  in strength. The evolution of these magnetic spots is simulated in a model. Star formation in the galactic disk causes—via supernova explosions—continuous injection of turbulent magnetic fields. Hence, the interaction of magnetic fields generated by small-scale dynamo action in discrete star formation regions was combined with the large-scale dynamo action [50]. Assuming that the injection of small-scale fields is situated only within the gaseous spiral arm regions where star formation mostly occurs, Moss et al. [48] obtained field structures with magnetic arms located between the spiral arms, as discussed in Section 3 (see Figure 5, right). Charmandy et al. [51] obtained similar results by considering that the galactic fountain flow or wind is likely to be weaker in the inter-arm regions than in the spiral arms.

## 6. Vertical Scale Heights and Galactic Wind

If synchrotron emission is the dominant loss process of the relativistic electrons in the halo, the outer shape of the radio emission should be dumbbell-like as synchrotron losses depend on the total magnetic field strength, which is stronger in the central region of a galaxy. In fact, a dumbbell shape of the total radio intensity was observed in some edge-on galaxies, e.g., NGC 253 [38] and NGC 891 [39]. As long as Inverse Compton (IC) radiation losses with Cosmic Microwave Background (CMB) photons are negligible ( $B > 3.25 \mu\text{G}$ ), synchrotron losses are the dominant radiation losses. The synchrotron lifetime  $t_{syn}$  at a fixed frequency is proportional to the total magnetic field strength  $B_t^{-1.5}$ . A cosmic ray bulk speed (velocity of a galactic wind) can be defined as  $v_{CR} = h_{CR}/t_{syn}$  with  $h_{CR}$  being the exponential scale height of the cosmic rays. The observed non-thermal intensity  $I_{syn} \propto N_0 B^{1+\alpha}$  with  $N_0 \propto N_{CR}$ , as shown in Formula (A3) by Beck & Krause [14] with  $N_{CR}$  being the total number density of cosmic ray particles and  $\alpha$  the non-thermal spectral index. The assumption of equipartition implies  $N_{CR} \propto B^2$  that leads to  $h_{CR} \propto (3 + \alpha)/2 \cdot h_{syn} \simeq 2h_{syn}$ , hence  $v_{CR} \simeq 2h_z/t_{syn}$  where  $h_z$  is the exponential scale heights of the observed radio emission. For NGC 253, Heesen et al. [38] determined the cosmic ray velocity to  $300 \pm 30 \text{ km/s}$  in the northeastern halo. As this is similar to the escape velocity from the disk, it shows the presence of a galactic wind in NGC 253. Meanwhile, the existence

of a galactic wind is also indicated for NGC 4631 [30] and a number of other galaxies by the 1D CR transport modelling SPINNAKER [39,40,52,53].

The observed extent of the radio emission of a galaxy may depend on the sensitivity of the radio map as more sensitive radio observations may permit to detect fainter regions. Instead, a vertical scale height as derived by an exponential or Gaussian fit to the vertical intensity distribution of the total radio emission is less affected by the sensitivity of the observations and hence a better indicator for the physics within the galaxy and a crucial parameter for understanding the transport of cosmic rays (CR) from the disk into the halo and the energy loss mechanisms of the cosmic ray electrons (CRE) within the halo of spiral galaxies. Until recently, radio scale heights could only be determined for a few bright and extended (i.e., nearby) spiral galaxies [22,53,54]. With the CHANG-ES observations of 35 edge-on spiral galaxies, we significantly increased the number and distance-range of the observed edge-on galaxies, as well as the sensitivity and angular resolution of the radio maps. Krause et al. [55] defined a subsample of 13 CHANG-ES galaxies that are small enough in angular size to be free of significant missing flux density by the interferometer observations. We determined the radio scale heights with exponential fits to the total intensity emission based on the method by Dumke et al. [56] but in a more sophisticated way [57]. Hence, we obtained for the first time radio scale heights of such a large sample of edge-on spiral galaxies in a consistent way. The sample average values for the halo scale heights are  $1.1 \pm 0.3$  kpc in C-band and  $1.4 \pm 0.7$  kpc in L-band [55].

Surprisingly, we detected that the halo scale heights increase linearly with the radio diameters as determined from our maps observed with similar sensitivity and also with the radio scale lengths, i.e., exponential fits to the radial total intensity distribution. We could, however, not find a clear correlation with the magnetic field strength, the SFR or star formation rate density (SFRD). In the discussion of that paper, we stated that we could not find an obvious physical explanation for the correlation of the halo scale heights with radio diameter that would not simultaneously imply a correlation of the halo scale height with star formation [55]. Meanwhile, Vargas et al. [58] developed a different calibration for the mid-IR extinction correction of  $H_\alpha$  luminosities to calculate the SFR in edge-on galaxies. This turned out to be necessary for edge-on galaxies because of the stronger  $H_\alpha$  extinction due to the long line-of-sight through the disk. With these updated  $SFR_{revised}$  values, they indeed obtained for the first time a correlation between radio scale heights and  $SFR_{revised}$ . They also observed a correlation of  $SFR_{revised}$  with radio diameters and radio scale lengths implying that the scale height—radio diameter correlation detected by Krause et al. [55] originates from the star formation in the disk.

The sample galaxies are consistent with an escape-dominated radio halo with convective cosmic ray propagation, indicating that galactic winds are a widespread phenomenon in spiral galaxies. A galactic wind may be essential for the formation of large-scale magnetic field in the halo, as discussed in Section 4. Indeed, model calculations of the mean-field  $\alpha - \Omega$  dynamo for a disk surrounded by a spherical halo including a galactic wind [59,60] simulated similar magnetic field configurations to the observed ones. Meanwhile, MHD simulations of disk galaxies including a galactic wind implicitly may explain the X-shaped field [61,62]. The first global, galactic scale MHD simulations of a CR-driven dynamo give promising results resembling the observations and show directly that small scale magnetic flux is transported from the disk into the halo [63]. A galactic wind can also solve the helicity problem of dynamo action (e.g., [51,64]). Hence, a galactic wind may be essential for an effective dynamo action and the observed X-shaped magnetic field structure in edge-on galaxies.

There are, however, also galaxies found for which Gaussian fits describe the vertical intensity distribution better than exponential fits, e.g., NGC 7462 [53] and NGC 4565 [39]. Their CR transport seems to be diffusion dominated as indicated by SPINNAKER [53].

When removing the scale height ( $h$ )—radio diameter ( $d_r$ ) dependence by introducing the normalized scale height  $\tilde{h} = 100 \cdot h/d_r$ , we found an anti-correlation of  $\tilde{h}$  with the mass surface density MSD [55]. This is the first observational evidence for a gravitational deceleration of the CRE outflow from the galactic disk [55]. Posterior observations [30,39,40] increasing the MSD range even

strengthen this result, as shown in Figure 6. Note that the two outliers NGC 4565 and UGC 10288 have a significantly lower magnetic field strength than the other galaxies, which may indicate an important role of the magnetic field strength on the CR outflows.

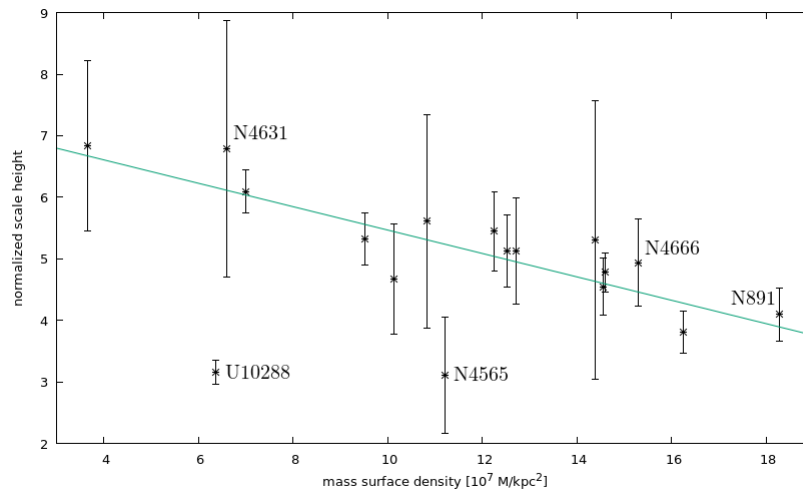


**Figure 6.** The normalized scale heights anti-correlate with the mass surface densities for the galaxies of the sample of Krause et al. [55], as well as for NGC 4666 [40], NGC 4631 [30], and NGC 891 [39]. The outliers (NGC 4565 and UGC 10288) have a significantly lower total magnetic field strength of only  $\approx 6 \mu\text{G}$ .

## 7. Conclusions

With radio continuum and linear polarization observations, we analyzed the magnetic field strength and structure in the disk and halo of spiral galaxies. Besides a turbulent magnetic field, a plane-parallel, spiral regular magnetic field was detected in the disks of all spiral galaxies observed, which is mainly axisymmetric (ASS) in most of the galaxies. Such a field structure corresponds to the solution of the fastest growing mode of a large-scale  $\alpha - \Omega$  dynamo operating in the disk. Models have been developed that can explain the magnetic field growing in strength and structure from the beginning of galaxy evolution at high  $z$  values. The magnetic field strength was mainly amplified by the turbulent dynamo, while the large-scale dynamo was mainly responsible for field ordering. Star formation plays an important role in these processes in accordance with the observations.

The halos of spiral galaxies, as the interfaces between the bright disk of the galaxy and the intergalactic medium, are less understood up to now. Recent detections of large-scale fields there (in addition to ordered and turbulent magnetic fields) cannot be explained by the  $\alpha - \Omega$  dynamo action in the disk alone. Increasing observational evidence for the existence of a CR-driven wind from the disk in the halo support the view that magnetic fields of all scales are transported into the halo by a galactic wind and can simultaneously solve the helicity problem of dynamo action in the disk. In addition, dynamo action in the halo remains possible. From the observational side, the structure of the large-scale fields in the halo has to be revealed by a careful analysis of the current data. Up to now, giant magnetic ropes (GMRs) could be identified in the halo of NGC 4631. If we want to trace the halo and magnetic fields further into the outer halo, more sensitive polarization data will be necessary. As Faraday depolarization effects are expected to decrease with increasing distance from the galactic disk, observations even in the decimeter wavelength regime with Meerkat and especially the SKA will be essential.

**Funding:** This research received no external funding.

**Acknowledgments:** The author thanks Rainer Beck for discussions and carefully reading the manuscript.

**Conflicts of Interest:** The author declares no conflict of interest.

## References

1. Avillez, M.A.; Breitschwerdt, D. Global Dynamical Evolution of the ISM in Star Forming Galaxies. I. High Resolution 3D Simulations: Effect of the magnetic Field. *Astron. Astrophys.* **2019**, *436*, 585–600. [[CrossRef](#)]
2. Korpi, M.J.; Brandenburg, A.; Shukurov, A.; Tuominen, I.; Nordlund, A. A Supernova-regulated Interstellar Medium: Simulations of the turbulent multiphase Medium. *Astrophys. J.* **1999**, *514*, L99–L102. [[CrossRef](#)]
3. Pakmor, R.; Springel, V. Simulations of Magnetic Fields in isolated Disc Galaxies. *Mon. Not. R. Astron. Soc.* **2013**, *432*, 176–193. [[CrossRef](#)]
4. Beck, R. Magnetism in the Spiral Galaxy NGC 6946: Magnetic Arms, depolarization Rings, dynamo Modes, and helical Fields. *Astron. Astrophys.* **2007**, *470*, 539–556. [[CrossRef](#)]
5. Tabatabaei, F.S.; Krause, M.; Fletcher, A.; Beck, R. High-resolution radio continuum Survey of M 33. III. Magnetic Fields. *Astron. Astrophys.* **2008**, *490*, 1005–1017. [[CrossRef](#)]
6. Marinacci, F.; Vogelsberger, M.; Pakmor, V.; Torrey, P.; Springel, V.; Hernquist, L.; Nelson, D.; Weinerger, R.; Pillepich, A.; Naiman, J.; et al. First Results from the IllustrisTNG Simulations: Radio Haloes and magnetic Fields. *Mon. Not. R. Astron. Soc.* **2018**, *480*, 5113–5139. [[CrossRef](#)]
7. Grand, R.J.J.; Gómez, F.A.; Marinacci, F.; Pakmor, R.; Springel, V.; Campbell, D.J.R.; Frenk, C.S.; Jenkins, A.; White, S.D.M. The Auriga Project: The Properties and Formation Mechanisms of Disc Galaxies across cosmic Time. *Mon. Not. R. Astron. Soc.* **2017**, *467*, 179–207. [[CrossRef](#)]
8. Pakmor, R.; Gómez, F.A.; Grand, R.J.J.; Marinacci, F.; Simpson, C.M.; Springel, V.; Campbell, D.J.R.; Frenk, C.S.; Guillet, T.; Pfrommer, C.; et al. Magnetic field Formation in the Milky Way like disc Galaxies of the Auriga Project. *Mon. Not. R. Astron. Soc.* **2017**, *469*, 3185–3199. [[CrossRef](#)]
9. Burn B.J. On the Depolarization of discrete Radio Sources by Faraday Dispersion. *Mon. Not. R. Astron. Soc.* **1966**, *133*, 67–83. [[CrossRef](#)]
10. Sokoloff, D.D.; Bykov, A.A.; Shukurov, A.; Berkhuijsen, E.M.; Beck, R.; Poezd, A.D. Depolarization and Faraday Effects in Galaxies. *Mon. Not. R. Astron. Soc.* **1998**, *299*, 189–206. [[CrossRef](#)]
11. Mora, S.C.; Krause, M. Magnetic Field Structure and Halo in NGC 4631. *Astron. Astrophys.* **2013**, *560*, A42. [[CrossRef](#)]
12. Brentjens, M.A.; de Bruyn, A.G. Faraday Rotation Measure Synthesis. *Astron. Astrophys.* **2005**, *441*, 1217–1228. [[CrossRef](#)]
13. Heald, G.; Braun, R.; Edmonds, R. The Westerbork SINGS Survey. II Polarization, Faraday Rotation, and magnetic Fields. *Astron. Astrophys.* **2009**, *503*, 409–435. [[CrossRef](#)]
14. Beck, R.; Krause, M. Revised Equipartition and minimum Energy Formula for magnetic Field Strength Estimates from radio Synchrotron Observations. *Astron. Nachr.* **2005**, *326*, 414–427. [[CrossRef](#)]
15. Niklas, S. Eigenschaften von Spiralgalaxien im hochfrequenten Radiokontinuum. Ph.D. Thesis, University Bonn, Bonn, Germany, 1995.
16. Fletcher, A.; Beck, R.; Shukurov, A.; Berkhuijsen, E.M.; Horrelou, C. Magnetic Fields and spiral Arms in the Galaxy M51. *Mon. Not. R. Astron. Soc.* **2011**, *412*, 2396–2416. [[CrossRef](#)]
17. Mulcahy, D.D.; Beck, R.; Heald, G.H. Resolved magnetic Structures in the disk-halo Interface of NGC 628. *Astron. Astrophys.* **2017**, *600*, A6. [[CrossRef](#)]
18. Krause, M. High Resolution Observations of the Magnetic Field in IC 342. In *The Cosmic Dynamo, Proceedings of IAU Symposium*; Cambridge University Press: Cambridge, UK, 1993; pp. 305–310.
19. Beck, R. Magnetic Fields in the nearby spiral Galaxy IC 342: A multi-frequency radio polarization Study. *Astron. Astrophys.* **2015**, *578*, A93. [[CrossRef](#)]
20. Beck, R.; Brandenburg, A.; Moss, D.; Shukurov, A.; Sokoloff, D. Galactic Magnetism: Recent Developments and Perspectives. *Annu. Rev. Astron. Astrophys.* **1996**, *34*, 155–206. [[CrossRef](#)]
21. Niklas, S.; Beck, R. A new Approach to the radio-far infrared Correlation for non-calorimeter Galaxies. *Astron. Astrophys.* **1997**, *320*, 54–64.
22. Krause, M. Magnetic Fields and Star Formation in Spiral Galaxies. *Rev. Mex. Astron. Astrofis.* **2009**, *36*, 25–29.
23. Stil, J.M.; Krause, M.; Beck, R.; Taylor, A.R. The integrated Polarization of spiral Galaxy Disks. *Astrophys. J.* **2009**, *693*, 1392–1403. [[CrossRef](#)]
24. Chyży, K.T. Magnetic Fields and Gas in the cluster-influenced spiral Galaxy NGC 4254. II. Structures of magnetic Fields. *Astron. Astrophys.* **2008**, *482*, 755–769. [[CrossRef](#)]

25. Frick, P.; Stepanov, R.; Beck, R.; Sokoloff, D.; Shukurov, A.; Ehle, M.; Lundgren, A. Magnetic and gaseous spiral Arms in M83. *Astron. Astrophys.* **2016**, *585*, A21. [[CrossRef](#)]
26. Berkhuisen, E.M.; Urbanik, M.; Beck, R.; Han, J.L. Radio Polarization and magnetic Field Structure in M 101. *Astron. Astrophys.* **2016**, *588*, A114. [[CrossRef](#)]
27. Ruzmaikin, A.A.; Shukurov, A.M.; Sokoloff, D.D. *Magnetic Fields of Galaxies*; Kluwer Academic Publishers: Dordrecht, The Netherlands, 1988.
28. Seigar, M.S.; Kennefick, D.; Kennefick, J.; Lacy, C.H.S. Discovery of a Relationship between Spiral Arm Morphology and Supermassive Black Hole Mass in Disk Galaxies. *Astrophys. J.* **2008**, *678*, L93–L96. [[CrossRef](#)]
29. Soida, M.; Krause, M.; Dettmar, R.-J.; Urbanik, M. The large scale magnetic Field Structure of the Spiral Galaxy NGC 5775. *Astron. Astrophys.* **2011**, *531*, A127. [[CrossRef](#)]
30. Mora-Partiarroyo, S.C.; Krause, M.; Basu, A.; Beck R.; Wiegert T.; Irwin, J.; Henriksen, R.; Stein, Y.; Vargas, C.J.; Heesen, V.; et al. CHANG-ES XIV: Cosmic-Ray Propagation and Magnetic Field Strengths in the Radio Halo of NGC 4631. *Astron. Astrophys.* **2019**, submitted.
31. Irwin, J.; Beck, R.; Benjamin, R.A.; Dettmar, R.-J.; English, J.; Heald, G.; Henriksen, R.N.; Johnson, M.; Krause, M.; Li, J.-T.; et al. Continuum Halos in Nearby Galaxies: An EVLA Survey (CHANG-ES). I. Introduction to the Survey. *Astron. J.* **2012**, *144*, 43. [[CrossRef](#)]
32. Irwin, J.; Damas-Segovia, A.; Krause, M.; Miskolczi, A.; Li, J.-T.; Stein, Y.; English, J.; Henriksen, R.; Beck, R.; Wiegert, T.; et al. CHANG-ES: XVIII—The CHANG-ES survey and relected results. *Galaxies* **2019**, *7*, 42. [[CrossRef](#)]
33. Krause, M.; Mora-Partiarroyo, S.C.; Schmidt, P. Magnetic Fields and CR Propagation in the Halos of Spiral Galaxies. In Proceedings of Focus Meeting 8 at the XXXth IAU General Assembly, Vienna, Austria, 29–31 August 2018; pp.127–128.
34. Mora-Partiarroyo, S.C.; Krause, M.; Basu, A.; Beck R.; English, J.; Wiegert T.; Irwin, J.; Henriksen, R.; Stein, Y.; Vargas, C.J.; et al. CHANG-ES XV: Large-Scale Magnetic Field Reversal in the Halo of NGC 4631. *Astron. Astrophys.* **2019**, submitted.
35. Woodfinden, A.; Henriksen, R.N.; Irwin, J.; Mora-Partiarroyo, S.C.; Evolving Galactic Dynamos and Fits to the Reversing Magnetic Field in the Halo of NGC 4631. *Mon. Not. R. Astron. Soc.* **2019**, submitted.
36. Moss, D.; Sokoloff, D. Magnetic Fields around galactic Discs. *Galaxies* **2019**, *7*, 36. [[CrossRef](#)]
37. Seta, A.; Beck, R. Revisiting the Equipartition Assumption in star-forming Galaxies. *Galaxies* **2019**, *7*, 45. [[CrossRef](#)]
38. Heesen, V.; Beck, R.; Krause, M.; Dettmar, R.-J. Cosmic Rays and the magnetic Field in the nearby Starburst Galaxy NGC 253. I. The Distribution and Transport of Cosmic Rays. *Astron. Astrophys.* **2009**, *494*, 563–577. [[CrossRef](#)]
39. Schmidt, P.; Krause, M.; Heesen, V.; Basu, A.; Beck, R.; Wiegert, T.; Irwin, J.A.; Heald, J.; Rand, R.J.; Li, J.-T.; et al. CHANG-ES XVI: An in-depth View of the Cosmic-Ray Transport in the edge-on Spiral Galaxies NGC 891 and NGC 4565. *Astron. Astrophys.* **2019**, submitted.
40. Stein, Y.; Dettmar, R.-J.; Irwin, J.; Beck, R.; Weżgowiec, M.; Miskolczi, A.; Krause, M.; Heesen, V.; Wiegert, T.; Heald, G.; et al. CHANG-ES XIII: Transport Processes and the magnetic Fields of NGC 4666—Indication of a reversing Disk magnetic Field. *Astron. Astrophys.* **2019**, *623*, A33. [[CrossRef](#)]
41. Stein, Y.; Dettmar, R.-J.; Weżgowiec, Irwin, J.; Beck, R.; Wiegert, T.; Krause, M.; Li, J.-T.; Heesen, V.; Miskolczi, A.; et al. CHANG-ES XIX: The Galaxy NGC 4013—A Diffusion-dominated Radio Halo with Plane-parallel Disk and Vertical Halo Magnetic Fields. *Astron. Astrophys.* **2019**, submitted.
42. Beck, R.; Poezd, A.D.; Sukurov, A.; Sokoloff, D.D. Dynamos in evolving Galaxies. *Astron. Astrophys.* **1994**, *289*, 94–100
43. Chamandy, L.; Taylor, A.R. Non-linear galactic Dynamos and the magnetic pitch Angle. *Astrophys. J.* **2015**, *808*, 28. [[CrossRef](#)]
44. Fletcher, A. Magnetic Fields in Nearby Galaxies. *Dynamoc Interstellar Medium Celebr. Can. Galactic Plane Surv.* **2010**, *438*, 197–210.
45. Beck, R. Magnetic Fields in spiral Galaxies. *Astron. Astrophys. Rev.* **2016**, *24*, 4. [[CrossRef](#)]
46. Arshakian, T.G.; Beck, R.; Krause, M.; Sokoloff, D. Evolution of magnetic Fields in Galaxies and future observational Tests with the Square Kilometre Array. *Astron. Astrophys.* **2009**, *494*, 21–32. [[CrossRef](#)]
47. Rodrigues, L.F.S.; Chamandy, L.; Shukurov, A.; Baugh, C.M.; Taylor, A.R. Evolution of galactic magnetic Fields. *Mon. Not. R. Astron. Soc.* **2019**, *483*, 2424–2440. [[CrossRef](#)]

48. Moss, D.; Beck, R.; Sokoloff, D.; Stepanov, R.; Krause, M.; Arshakian, T.G. The Relation between magnetic and material Arms in Models for Spiral Galaxies. *Astron. Astrophys.* **2013**, *556*, A147. [[CrossRef](#)]
49. Arshakian, T.G.; Stepanov, R.; Beck, R.; Krause, M.; Sokoloff, D. Modeling the total and polarized Emission in evolving Galaxies: “Spotty” magnetic Structures. *Astron. Nachr.* **2011**, *332*, 524–536 [[CrossRef](#)]
50. Moss, D.; Stepanov, R.; Arshakian, T.; Beck, R.; Krause, M.; Sokoloff, D. Multiscale magnetic Fields in Spiral Galaxies: Evolution and Reversals. *Astron. Astrophys.* **2012**, *537*, A68. [[CrossRef](#)]
51. Chamandy, L.; Shukurov, A.; Subramanian, K. Magnetic spiral Arms and galactic Outflows. *Mon. Not. R. Astron. Soc.* **2015**, *446*, L6–L10. [[CrossRef](#)]
52. Heesen, V.; Krause, M.; Beck, R.; Adebahr, B.; Bomans, D.J.; Carretti, E.; Dumke, M.; Heald, G.; Irwin, J.; Koribalski, B.; et al. Radio Haloes in nearby Galaxies modelled with 1D Cosmic Ray Transport using SPINNAKER. *Mon. Not. R. Astron. Soc.* **2018**, *476*, 158–183 [[CrossRef](#)]
53. Heesen, V.; Dettmar, R.-J.; Krause, M.; Beck, R. Advective and diffusive Cosmic Ray Transport in galactic Haloes. *Mon. Not. R. Astron. Soc.* **2016**, *458*, 332–353. [[CrossRef](#)]
54. Dumke, M.; Krause, M. Radio and Polarization Properties in the Disk and Halo of edge-on Spirals. In *IAU Colloq. 166: The Lokal Bubble and Beyond*; Lecture Notes in Physics; Springer: Berlin, Germany, 1998; pp. 555–558.
55. Krause, M.; Irwin, J.; Wiegert, T.; Miskoczi, A.; Damas-Segovia, A.; Beck, R.; Li, J.-T.; Heald, G.; Müller, P.; Stein, Y.; et al. CHANG-ES. IX. Radio Scale Heights and Scale Lengths of a consistent Sample of 13 Spiral Galaxies seen edge-on and their Correlations. *Astron. Astrophys.* **2018**, *611*, A72. [[CrossRef](#)]
56. Dumke, M.; Krause, M.; Wielebinski, R.; Klein, U. Polarized Radio Emission at 2.8cm from a selected Sample of edge-on Galaxies. *Astron. Astrophys.* **1995**, *302*, 691–703.
57. Müller, P.; Krause, M.; Beck, R. The NOD3 Software Package: A graphical user Interface-supported Reduction Package for Single-Dish Radio Continuum and Polarisation Observations. *Astron. Astrophys.* **2017**, *606*, A41. [[CrossRef](#)]
58. Vargas, C.J.; Walterbos, R.A.M.; Rand, R.J.; Stil, J.M.; Krause, M.; Li, J.-T.; Irwin, J. CHANG-ES XVII: H $\alpha$  Imaging of Nearby Edge-on Galaxies, New SFRs, and an Extreme Star Formation Region—Data Release 2. *Astrophys. J.* **2019**, submitted.
59. Brandenburg, A.; Donner, K.J.; Moss, D.; Shukurov, A.; Sokoloff, D.; Tuominen, I. Vertical magnetic Fields above the Discs of Spiral Galaxies. *Astron. Astrophys.* **1993**, *271*, 36–50.
60. Moss, D.; Sokoloff, D.; Beck, R.; Krause, M. Galactic Winds and the Symmetry Properties of galactic magnetic Fields. *Astron. Astrophys.* **2010**, *512*, A61. [[CrossRef](#)]
61. Gressel, O.; Elstner, D.; Ziegler, U.; Rüdiger, G. Direct Simulations of a Supernova-driven galactic Dynamo. *Astron. Astrophys.* **2008**, *486*, L35–L38. [[CrossRef](#)]
62. Hanasz, M.; Otmianowska-Mazur, K.; Kowal; Lesch, H. Cosmic-Ray-driven Dynamo in galactic Disks. A Parameter Study. *Astron. Astrophys.* **2009**, *498*, 335–346. [[CrossRef](#)]
63. Hanasz, M.; Wóltanski, D.; Kowalik, K. Global galactic Dynamo driven by Cosmic Rays and exploding magnetized Stars. *Astrophys. J.* **2009**, *706* L155–L159. [[CrossRef](#)]
64. Sur, S.; Shukurov, A.; Subramanian, K. Galactic Dynamos supported by magnetic Helicity Fluxes. *Mon. Not. R. Astron. Soc.* **2007**, *377*, 874–882. [[CrossRef](#)]

